Journal of Hydrology 490 (2013) 88–105

Contents lists available at SciVerse ScienceDirect

Journal of Hydrology

journal homepage: www.elsevier.com/locate/jhydrol

Assessing the impact of climate and land use changes on extreme floods in a large tropical catchment

Chatchai Jothityangkoon [a,*], Chow Hirunteeyakul [a], Kowit Boonrawd [a], Murugesu Sivapalan [b,c]

[a] School of Civil Engineering, Suranaree University of Technology, 111 University Avenue, Muang District, Nakhon Ratchasima 30000, Thailand
[b] Departments of Geography and Geographic Information Science, University of Illinois at Urbana-Champaign, 220 Davenport Hall, 607 S. Mathews Avenue, Urbana, IL 61801, USA
[c] Department of Civil and Environmental Engineering, University of Illinois at Urbana-Champaign, 220 Davenport Hall, 607 S. Mathews Avenue, Urbana, IL 61801, USA

ARTICLE INFO

Article history:
Received 26 November 2012
Received in revised form 11 March 2013
Accepted 22 March 2013
Available online 2 April 2013
This manuscript was handled by Konstantine P. Georgakakos, Editor-in-Chief, with the assistance of Attilio Castellarin, Associate Editor

Keywords:
Probable Maximum Precipitation (PMP)
Probable Maximum Flood (PMF)
Rainfall–runoff model
Compound channel
Dam safety

SUMMARY

In the wake of the recent catastrophic floods in Thailand, there is considerable concern about the safety of large dams designed and built some 50 years ago. In this paper a distributed rainfall–runoff model appropriate for extreme flood conditions is used to generate revised estimates of the Probable Maximum Flood (PMF) for the Upper Ping River catchment (area 26,386 km^2) in northern Thailand, upstream of location of the large Bhumipol Dam. The model has two components: a continuous water balance model based on a configuration of parameters estimated from climate, soil and vegetation data and a distributed flood routing model based on non-linear storage–discharge relationships of the river network under extreme flood conditions. The model is implemented under several alternative scenarios regarding the Probable Maximum Precipitation (PMP) estimates and is also used to estimate the potential effects of both climate change and land use and land cover changes on the extreme floods. These new estimates are compared against estimates using other hydrological models, including the application of the original prediction methods under current conditions. Model simulations and sensitivity analyses indicate that a reasonable Probable Maximum Flood (PMF) at the dam site is 6311 m^3/s, which is only slightly higher than the original design flood of 6000 m^3/s. As part of an uncertainty assessment, the estimated PMF is sensitive to the design method, input PMP, land use changes and the floodplain inundation effect. The increase of PMP depth by 5% can cause a 7.5% increase in PMF. Deforestation by 10%, 20%, 30% can result in PMF increases of 3.1%, 6.2%, 9.2%, respectively. The modest increase of the estimated PMF (to just 6311 m^3/s) in spite of these changes is due to the factoring of the hydraulic effects of trees and buildings on the floodplain as the flood situation changes from normal floods to extreme floods, when over-bank flows may be the dominant flooding process, leading to a substantial reduction in the PMF estimates.

1. Introduction

Most existing large dams in Thailand and in many other countries were designed and constructed during the 1960–1980 period, making them now 30–50 years old. After such long periods of operation has come the realization that physical characteristics of the catchment area of these dams may have significantly changed due to human activities: increase of population leading to increased deforestation and the expansion of both agricultural and urban areas, possible increases in rainfall due to natural climate variability or climate change caused by the greenhouse effect. Flood disasters have been reported in many regions and countries, in many cases the observed magnitudes and frequency of many contemporary floods have been found to be more severe than in the observed record (Brakenridge, 2013; Pinter et al., 2006a,b; Syvitski and Brakenridge, 2013). A major question has arisen in the public mind as to whether the dams remain safe under these changed circumstances. Questions are also being raised by dam safety operators as to whether the spillway capacities of the dams are sufficient for the magnitudes and frequency of current and future flooding. In Thailand these concerns have been brought to a head in the wake of the devastating floods that occurred in 2011 and inundated much of the floodplain of the Chao Phraya River. To find reasonable answers to these questions, there is an urgent need to revise the methods used for estimating the design flood, using the current and future conditions that may be operating within the catchment area.

The design flood we are interested in here is the extreme flood, i.e., the so-called Probable Maximum Flood (PMF), which is defined as the "largest flood that can reasonably be expected to occur on a given stream at a selected point" (United States Department of the Interior, Bureau of Reclamation, 1974). Normally, the PMF is estimated by transforming the Probable Maximum Precipitation

* Corresponding author. Tel.: +66 44 22 4426; fax: +66 44 22 4607.
E-mail address: cjothit@sut.ac.th (C. Jothityangkoon).

0022-1694/$ - see front matter © 2013 Elsevier B.V. All rights reserved.
http://dx.doi.org/10.1016/j.jhydrol.2013.03.036

(PMP). The focus of the present study is on the Upper Ping River catchment (26,386 km^2) upstream of the large Bhumipol Dam in northern Thailand. However, the issues discussed apply to any other large dam in any other part of the world, especially those that were designed and built in the 1950–1960 period. Chao et al. (2008) compiled a database of world dams from the International Commission on Large Dames. For the world's largest dams by volume greater than 29 km^3 only, 13 of 46 dams (28%) have been operated since 1964, and are of the same age as the Bhumipol Dam. Design flood criteria of these old dams are likely to be the same as those for the Bhumipol Dam, and estimated based on flood frequency analysis or/and lumped unit hydrograph method. Hundreds of dams around the world constructed around the same time could be in need of reassessment for safety as they may not have been designed using current updated PMF procedures (Graham, 2000).

There is considerable uncertainty about sufficiency of the design flood estimates upon which they were constructed. Estimation procedures for PMP have been revised in the intervening 50 years. There is considerable concern about changes to PMP estimates as a result of natural climate variability and climate changes associated with the greenhouse effect. As part of the population growth there have been considerable expansion of agriculture and urbanization, and associated land use and land cover changes, which can be expected to have a significant impact on the runoff processes and therefore the PMF. All of these factors can potentially contribute to an increase in the extreme flood estimates. Opposed to these obvious increases is the fact that there have also been improvements in our understanding of the rainfall–runoff and flooding processes, including extreme flood processes. The improved methods based on the actual dominant processes that operate under extreme flood conditions are now available and can simulate more realistically than before (i.e. Jothityangkoon and Sivapalan, 2003). The proposed modifications to the design and operation of an existing dam to account for these changed circumstances and accommodate new estimates of the PMF requires a procedure for the evaluation of the costs and benefits (Graham, 2000). It is therefore important, and timely, that all of these are considered as part of the revision of the PMF estimates, including the associated uncertainties, so that dam safety operators can exercise judgment and make appropriate short term, medium term and long term strategic decisions regarding the operation of the dam as well as any upgrading of spillway capacities to mitigate the negative effects of a potentially extreme flood in the future. Based on these considerations the Electricity Generating Authority of Thailand (EGAT), the operator of many large dams in Thailand, has called for a revision of the design flood (i.e. PMF) for the Bhumipol Dam, which is the motivation for the work presented in this paper.

To address the questions as to whether many old dams are still safe and their spillway capacities are able to accommodate future extreme floods, existing spillway capacity based on old design flood criteria should be reexamined to identify the potential risk of failure caused by overtopping. The aims of this paper are: (1) develop an extreme flood estimation model based on the combination of a long-term water balance model and a distributed runoff-routing model representing flow processes in a compound channel, extending a previous model application in a semi-arid catchment of medium size (Jothityangkoon and Sivapalan, 2003) to, in this study, a larger tropical catchment; (2) to investigate the impact of climate and land use changes on extreme floods under different scenarios, involving different types or patterns of PMPs, antecedent moisture conditions, increased rainfall under climate change, and deforestation; (3) to understand the reasons behind the difference between the old design floods and recalculated design floods, (4) to identify the critical parameter and processes under extreme condition, that could potentially lead to a reduction of the PMF estimates and in this way lead to a reduction in the uncertainty of extreme flood estimates. The method proposed here is an example of the procedures that can be used in other countries, provided suitable adaptations are made to account for differences in meteorology and hydrology.

2. Overview of proposed revisions to PMP and PMF estimation

Example results of extreme flood estimation in Thailand are presented in Table 1, containing the magnitudes of the estimated PMFs for eight other large dams, excepting the Bhumipol Dam. This information was collected from design reports for each of the dams and a report from EGAT (1988). The Bhumipol Dam was built in 1964 and at that time only the observed maximum flood and rainfall were used in the estimation of design flood. Standard design procedures for estimating PMFs using PMPs were instituted after the Bhumipol Dam was designed and built. This is another reason that calls for careful examination of the safety of the Bhumipol Dam, not only using design procedures that are now standard, but also considering the changes that may have happened in the last 50 years to PMP estimates and land use and land cover changes, and also improved hydrological models that are appropriate under potential extreme flood conditions. The key areas that require updating and improvement are summarized below, along with approaches adopted in this paper.

2.1. Estimation of Probable Maximum Precipitation (PMP)

Hansen et al. (1982) has given a definition of the PMP as "theoretically the greatest depth of precipitation for a given duration that is physically possible over a given storm area at a particular geographical location at a certain time of the year". Based on this definition, there has been further development of PMP estimates in many countries: China (Daojiang and Jinshang, 1984), India (Rakhecha and Kennedy, 1985), Czech Republic (Rezacova et al., 2005), and USA (Hansen, 1987). Rezacova et al. (2005) produced statistical estimates of the design PMP of duration 1–5 days at rain gauge positions and then converted theses point PMPs to area averaged PMPs by using maximized area reduction factors (ARFs)

Table 1
Estimated floods for designing of eight large dams in Thailand, where PMF is the Probable Maximum Flood and PMP is the Probable Maximum Precipitation.

Parameters	Name of dams							
	Bhumipol	Sirikit	Srinagarin	Ubol Ratana	Khao Laem	Rajjaprabha	Bang Lang	Kaeng Sue Ten
PMF (m^3/s)	6000*	10,500	7100	17,631	7100	5320	6334	10,400
Recorded max. flood (m^3/s)	4500	5260	2867	6334	3146	1516	1850	–
PMP (mm)	380	360	350	478	587	1119	1056	624
Duration (days)	–	7	9	3	10	5	5	5
Drainage area (km^2)	26,386	13,130	10,880	12,000	3720	1435	2080	3850
Year of operation	1964	1974	1980	1966	1985	1987	1981	–

* Recommended maximum flood.

determined from radar-based rainfalls. Ohara et al. (2011) proposed a potential alternative to the estimation of PMPs using a physically based regional atmospheric model (namely, the MM5 model). This modeling approach can use synoptic atmospheric data from many sources, including general circulation model (GCM) climate projections.

In this study, the estimation of the new PMP values are obtained using two alternative methods, the brief details of which are presented next.

2.1.1. Statistical method

This method is useful for making quick estimates. The estimation procedure was developed by Hershfield (1961). Although this estimate is normally meant for small catchments, it can also be used for large catchments (World Meteorological Organization, WMO, 1986). The method involves the application of the Hershfield equation:

$$P_{\max} = [P_{mean,n}F_{11} + K_{\max}S_nF_{12}]F_2F_3 \quad (1)$$

where $P_{\max}$ = maximized daily rainfall (PMP), $P_{mean,n}$ = mean of annual maxima from n years, S_n = standard deviation estimated from the record, F_{11} = adjustment factor for $P_{mean,n}$ for length of record, F_{12} = adjustment factor for $P_{mean,n}$ for S_n, F_2 = adjustment factor for fixed observational time interval, and F_3 = adjustment factor for transition from point rainfall to areal rainfall. The parameters of Hershfield's equation are estimated based on statistical analysis of 24 h rainfall data.

2.1.2. Generalized method

Generalized or regional estimates can be presented in two formats. The first format is a series of isohyetal maps, each map depicting the geographic variation of PMP over the region for some specified duration and storm size, commonly known as generalized or regional charts of PMP and used in non-orographic regions. The second format presents a series of relationships which permit the user to develop a PMP estimate for any desired location. A number of index maps are used to depict the geographic variation, for a particular component or area size and duration of PMP. This format is commonly used where topography plays an important role in the precipitation process (WMO, 1986). Another approach, although not used in this study, is the use of a storm model. PMP estimation using the storm modeling approach uses a physical parameterization of precipitation processes and then on a maximization of the various components of the precipitation process.

2.2. Catchment hydrological model for PMF estimation

Hydrologic modeling is the common approach to estimate the extreme flood (PMF) on the basis of PMP estimates. In Thailand, the catchment flood routing model (i.e., the CFR model) was used by the Snowy Mountains Engineering Corporation (Mein et al., 1974). In Australia, the RORB runoff routing model of Laurenson et al. (2006) is recommended by the Australian Rainfall–Runoff guidelines (Institution of Engineers, 2001). In the Unites States, the HEC–HMS, HEC–RAS models and the Corps Water Management System (CWMS) are typically used by the US Army Corps of Engineers, and the flood hydrograph and runoff (i.e., FHAR) model is used by the Bureau of Reclamation (1990) for dam safety investigations. In the United Kingdom, the unit hydrograph method is specified in the national guidelines produced by the Institute of Hydrology (1999). Other methods for PMF estimation include frequency curve extension (Harris and Brunner, 2011), use of a dynamic-stochastic model and the fitting the simulated peak flows to the Johnson distribution (Kuchment and Gelfan, 2011), the use of a two dimensional, physically-based rainfall–runoff model (i.e., CASC2D) on a large watershed for dam safety risk analysis (England et al., 2005), and the inclusion of paleo-flood data in combination with flood frequency analysis (Jarrett and Tomlinson, 2000).

In general, hydrological models used for extreme flood estimation contain two major components: (i) a runoff generation component (or loss model) based on an initial loss followed by a continuing constant or variable loss rate applied to the PMP, (ii) a routing component based on unit hydrograph derived from observed rainfall–runoff analysis or a synthetic unit hydrograph regionalized from observations in other places, or a distributed runoff routing model over the river network.

2.2.1. Runoff generation or "loss" model

A range of model complexities could be considered for extreme flood estimation. However, parameter estimation is a serious concern in the case of extreme floods, which are far more extreme beyond what has been experienced in the observed record. There is often a tendency to estimate model parameters of the loss models on the basis of calibration with observed, and therefore less-than-extreme, floods. During the extrapolation to extreme floods, both observed flood events and the extreme flood event are assumed to be dominated by the same runoff generation and routing processes. Not considering the actual flood producing mechanisms that operate under extreme conditions may give rise to biased estimates of extreme floods. For example, dominant runoff generation processes can change from saturation excess overland flow to infiltration excess overland flow with increasing return period (Sivapalan et al., 1990; Wood et al., 1990), or from subsurface stormflow to saturation excess overland flow (Samuel and Sivapalan, 2008), and thus may impact the shape of the flood frequency curve. Knowing and using the potential dominant processes or mechanisms that actually operate during extreme floods is likely to improve extreme flood estimation.

The extreme flood model framework presented in this study is a continuation of that proposed by Jothityangkoon and Sivapalan (2003), which represents a significant advance over the previous approaches in a number of ways. Firstly, the runoff generation model is replaced by a continuous catchment water balance model that (a) includes saturation excess runoff and subsurface stormflow, and (b) can be applied to the large tropical catchment in this case with no or minimal calibration and can be used to simulate normal or observed flood events. Secondly, the soil parameters are estimated *a priori* based on field data and also the effects of antecedent soil wetness can be simulated internally, considering that it is a continuous water balance model. The model is run on a daily time step for long-term water balance estimation and to set up the antecedent soil moisture conditions for a given storm, and on an hourly time step for PMP–PMF event simulations.

2.2.2. Runoff routing under extreme flood conditions

Woltemade and Potter (1994) used the MIKE 11 rainfall–runoff hydrodynamic model to investigate the influence of geomorphic factors on flood peak attenuation and found that channel-floodplain-terrace morphology, valley width, stream slope and hydraulic roughness influence peak discharges for moderate flood magnitudes (5–50 years return period). Jothityangkoon and Sivapalan (2003) developed a rainfall–runoff model for extreme flood estimation for the Collie River basin in Western Australia, whose application demonstrated that when moving from normal floods to PMFs, the dominant runoff process in the stream channel changed from in-bank to over-bank flows, and that floodplain inundation and floodplain vegetation helped to significantly reduce the magnitude of the estimated PMFs.

The runoff routing component of the model proposed here divides the catchment into a network of non-linear storages associated with various river reaches. The storage–discharge

relationship used is $S = kQ^m$ where Q is discharge, S is storage in the stream, and k and m are model parameters, as in the RORB model. However, there are two main differences compared to previous models (e.g., RORB). Firstly, runoff contributions from sub-catchment area to the channel reaches are generated by the catchment water balance model. Secondly, the parameters k and m are estimated *a priori* based on physically realistic, hydraulic characterization of compound channels to capture the combined effects of in-bank flow and over-bank flow on the floodplains, whereas these parameters are usually estimated by calibration with observed less-than-extreme flood events in other models (e.g., RORB). The above features of the proposed model make it a more reliable tool for the estimation of extreme floods.

2.2.3. Accounting for land use changes

Previous experience with the Ubol Ratana Dam in another part of Thailand is instructive in regard to the potential effect of land use changes on extreme floods. A hydrological study for the Ubol Ratana Dam (i.e., Nam Pong project) was carried out in November 1963 by Salzgitter Industriebau GmbH (1963), based on which the original design capacity of the spillway was set at 2500 m^3/s. Later in 1978, after 12 years of operation, an extraordinary flood occurred that exceeded the spillway design capacity by 51% (i.e., 3775 m^3/s). The Ubol Ratana flood protection study was conducted again by Salzgitter Consult GmbH et al. (1983) to review the design criteria and to adjust the design flood. This study found that the annual runoff coefficient of the catchment had increased significantly from 0.18 (average obtained from the records over 1956–1962) to its peak of 0.40 by year 1980, whereas the value used in the original design was 0.26. The main cause of this remarkable increase of the annual runoff coefficient is the heavy deforestation that occurred within the catchment. The area denuded of the original forest cover over the 15-year period (1966–1980) was close to 70%, which was not foreseen during the original design in 1963. There is therefore reason to be concerned that a similar effect could occur at the Bhumipol Dam as well. The current recommended design maximum flood (PMF) for Upper Ping catchment at the site of the Bhumipol Dam is 6000 m^3/s. It was estimated by the Bureau of Reclamation (United States Department of the Interior) (1955), whereas an estimate based on the envelope curve of all maximum flood peaks previously experienced in Thailand was 4300 m^3/s (for a catchment of area 26,400 km^2). However, based on the experience at Ubol Ratana Dam, EGAT now suspects that current maximum floods in the Upper Ping catchment may possibly exceed the previously adopted design flood.

3. Application of extreme flood model to the Upper Ping catchment

3.1. Study catchment

The Ping river is one of four tributaries of the Chao Phraya river, the most important interior river of Thailand, that passes through the central region of the country and the capital city of Bangkok before discharging into the Gulf of Thailand. The Upper Ping river catchment is located in the northern region of Thailand (see Fig. 1). The Basin lies between the Wang and the Salween river basin of Burma (or Myanmar). The stream network of this basin is formed by several mountain ranges with a high elevation about 1500 m. The Tenasserim range stretches from the Shan states separating the Ping from Salween River. Descending from the high mountain ranges, the main stream of the Upper Ping River flows southward through the valley of Chiang Mai, one of the most popular tourist destinations of northern Thailand, and the Tak province, over a distance of about 390 km before arriving at the Bhumipol Dam. The catchment area upstream of Bhumipol Dam is 26,386 km^2 and maximum reservoir storage is 13,462 $\times$ 10^6 m^3. There are 90 well-distributed rain gauges inside and nearby the catchment. The longest record is 57 years (1951–2007) long. There are also 92 streamgauges. We selected a 24 year sequence of daily rainfall and runoff time series (1982–2005) during which most of the gauges were operational. Details of the hydrological data, topography, soil and vegetation of the Upper Ping catchment are summarized below.

3.1.1. Land use

The LANDSAT satellite images are used as an input for classification of the land use and land cover using a combination of GIS techniques and field surveys carried out with GPS. The analysis revealed that the percentage of forest, urban and plantations are 70%, 12%, and 6%, respectively.

3.1.2. Climate

The region is subjected to tropical climate with a long rainy season (May–October), short summer (March–April) and short winter (November–February). The long term areal averaged annual rainfall, potential evaporation and runoff for the Upper Ping catchment are 1174 mm, 1661 mm and 260 mm, respectively.

3.1.3. Topography, soils and landforms

The general topography of the catchment consists of steep and complex mountain ranges with elevation varying from 140 m to 2500 m (MSL). The majority of the soils within the catchment is classified as "slope complex" in the landform soils map, produced by the Land Development Department (LDD), Ministry of Agriculture and Cooperatives, Thailand. Previous studies on the Mae Chaem River catchment, a tributary of the Upper Ping, indicate that prevalent soil texture is sandy clay loam (Thanapakpawin et al., 2006), and deep clays (Croke et al., 2004). Soil profile data has been collected from the cores of 1166 deep artesian wells by the Department of Groundwater Resources, Thailand. Soil types and depths are, roughly recorded, in the range of 0–10 m from the surface. By overlying these wells on the landform maps, the distribution of soil depths was estimated for each landform, and used in the model development.

3.1.4. Vegetation

Over the forested parts of the catchment, vegetation is mainly dominated by mixed deciduous forest, hill evergreen forest and deciduous dipterocarp forest.

Previous studies in the Mae Chaem River catchment mainly focused on the effect of land use changes on runoff using different models. Croke et al. (2004) applied the IHACRES rainfall–runoff model to investigate the impacts of forest cover changes in Mae Chaem (A = 2157 km^2). Thanapakpawin et al. (2006) used the Distributed Hydrology-Soil Vegetation Model (DHSVM) to analyze the impacts of forest-to-crop conversion and vice versa, in Mae Chaem catchment (A = 3853 km^2).

3.2. Parameter estimation for PMP for the Upper Ping river

3.2.1. Statistical estimation

The PMP values of different durations are estimated by using observed rainfall data from raingauges. Four and eight main rain gauges with highly reliable quality of data in different provinces were selected with record lengths of 56 years (1951–2006) and 24 years (1982–2005), respectively. The statistics of annual maximum rainfall for three durations are presented in Table 2. These statistics combined with adjusted factors recommended by WMO (1986) are used to estimate the parameters involved in the statistical methods. The estimated PMP value of 1 day duration is

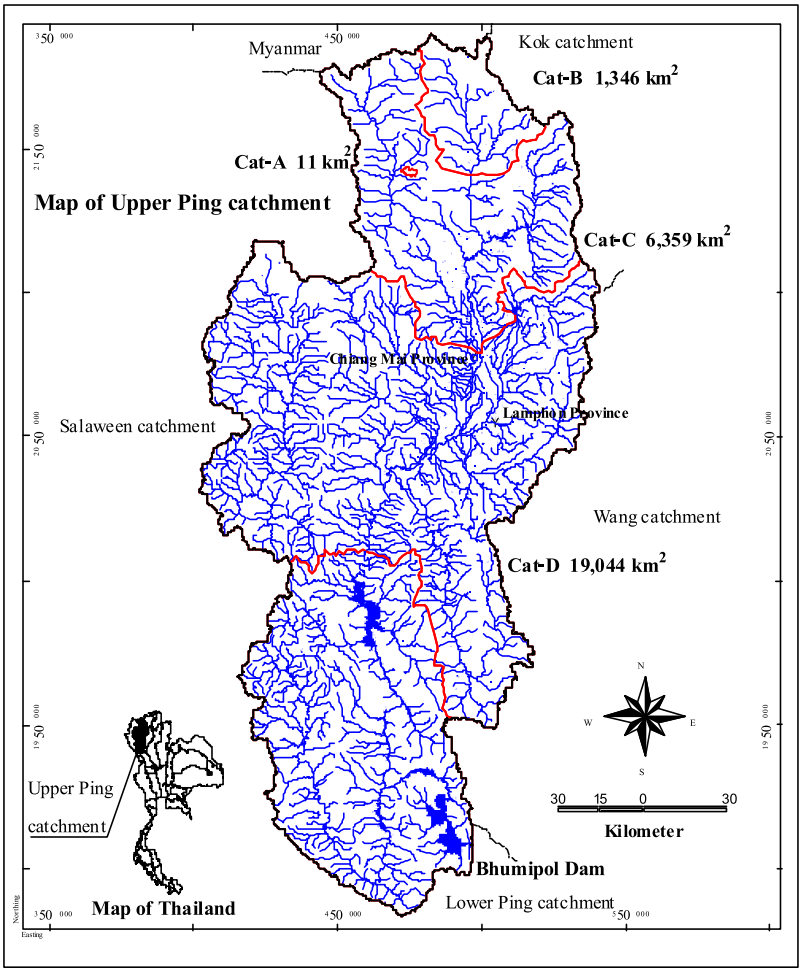

Fig. 1. Location map of study area, stream network and catchment and subcatchment boundaries of the Upper Ping River Basin, upstream of Bhumipol dam.

Table 2
Mean and standard deviation of areal maximum annual rainfall depth for 3 durations.

List of statistic parameters for each cases	Rainfall duration		
	1 day	2 day	3 day
Case 1: eight stations, year 1982–2005			
Mean (mm)	43.9	63.5	77.1
Standard deviation	11.7	16.8	18.4
Case 2: four stations, year 1951–2006			
Mean (mm)	77.6	98.4	113.3
Standard deviation	16.2	20.5	22.9

Table 3
Parameters for estimation of PMP with 1 day duration.

List of parameters	Values
Length of record (year)	56
$P_{mean,n}$ (mm)	77.6
S_n	16.2
K_{max} (WMO manual, Fig. 4.1)	16.1
F_{11} (WMO manual, Fig. 4.4)	1.00
F_{12} (WMO manual, Fig. 4.1)	1.00
F_2 (WMO manual, Page 100)	1.13
F_3	1.00
PMP 24 (mm)	382

382 mm. All parameter values and calculated PMP values are presented in Table 3.

3.2.2,. Generalized estimates from Mekong River basin

US Department of Commerce and US Department of the Army (1970) developed a generalized isohyets map of the lower Mekong River basin from basic 5000 km^2, 24 h depth-area-durations curve of Vietnam coast. We extrapolated these isohyets to the Upper Ping River catchment, which is near the Mekong River Basin and found that the appropriate PMP is about 400 mm. This previous study also provided depth-duration-area curves that can be applied to estimate 6–72 h duration PMPs in Upper Ping catchment (Table 4). The increase of PMP for each 6 h is rearranged, ranked, and regrouped to 3 days. Daily PMP from maximum to minimum values are 220 mm, 72 mm and 56 mm, respectively. The sequence of these daily PMPs is designed at a fixed maximum value on the second day. The time series of PMPs can be expressed in terms of two patterns (1) 72 mm, 220 mm, 56 mm and (2) 56 mm, 220 mm, 72 mm.

Table 4
Accumulated depth of estimated PMP for 6–72 h duration for the Upper Ping river basin.

Duration (h)	Accumulated PMP (%)	Accumulated PMP (mm)
6	23	92
12	35	140
18	47	188
24	55	220
48	73	292
72	87	348

Table 5
Design PMP for 2 cases based on Generalized estimates from the Mekong River basin and from observed extreme rainfall "Tilda" in Thailand.

Case no.	Day	Rank	PMP depth (mm)	
			Mekong	Tilda
1	1	2nd	36	32
	2	1st	110	81
	3	3rd	28	8
	4	3rd	56	17
	5	1st	220	161
	6	2nd	72	64
	Sum		522	363
2	1	2nd	47	42
	2	1st	143	105
	3	3rd	36	11
	4	Normal	0	0
	5	2nd	72	64
	6	1st	220	161
	7	3rd	56	17
	Sum		574	400

To formulate the design PMP storm, US Department of Commerce and US Department of the Army (1970) recommended that the time series of PMP storm events comprise a prior storm 50% of PMP or 65% of PMP in case the time lag between maximum daily PMP of prior and major PMP storms are 3 or 4 days (see Table 5). The isohyetal pattern proposed by WMO (1986) is applied to estimate the spatial distribution of rainfall in the study area by locating the center of the isohyetal pattern in the center of the study catchment and rotating the isohyetal pattern until the catchment receives maximum rainfall. US Department of Commerce and US Department of the Army (1970) provided the percentage of daily rainfall depth for each isohyetal line based on 6 h PMP, and in this way the depth distribution of spatial rainfall for the study catchment are estimated. The area enclosing isohyetal lines is measured and is used as a weighting factor multiplied by PMP depth for each isohyetal line. Areal averaged rainfall based on 6 h PMP was estimated to be 69.95 mm (i.e., 1,846,710/26,400).

3.2.3. Generalized estimates using observed severe storm in Thailand

From a previous study on the Nan River Basin (ECI Engineering Consultants Inc., 1969), the most severe Typhoon on 22–24 September 1964, called Tilda, centered at Roi-et province, was selected for analysis because it gave the maximum rainfall ever recorded in Thailand and this observation provided a complete record of isohyets and the storm route. The center of Tilda is transposed from Roi-et province to Upper Ping catchment. This transposition requires some adjustments for compensation of the difference of the climate and topography between the two locations.

The reference dew point temperature adjustment of maximum humidity for this region is not necessary, compared to a middle latitude region such as USA. Therefore, necessary humidity adjustment for the Upper Ping catchment is assumed to be +3% (US Department of Commerce and US Department of the Army, 1970). For the adjustment for distance inland, the US Department of Commerce and the US Department of the Army (1970) found that a tropical storm approaching from the east coast of Viet Nam and the tropical storm decreases when the storm moves further inland in a westward direction. The PMP of 72 h duration with a depth 1200 mm was estimated for the area along the coastline of Viet Nam, which decreased to 480 mm (40%) over the Roi-et province located towards the west of the Mekong River Basin. This estimated PMP depth is close to the observed maximum rainfall depth. ECI Engineering Consultants Inc. (1969) used a reduction factor of 10% for storm transposition of maximum rainfall from Roi-et province which is to the west of the Nan River Basin. We also used a reduction factor of 20% for storm transposition to the Upper Ping catchment due to it being located at double the distance to the west. For barrier adjustment, ECI Engineering Consultants Inc. (1969) estimated that rainfall depth decreases by 14% as a result of this dissipation. There is a mountain range between Nan River basin and Upper Ping River Basin, but its stretch is not continuous and its height is less than Luang Prabang. Therefore, barrier adjustment for storm transposition to Upper Ping River Basin is estimated to be 15%. There is no need for elevation and season adjustment. Table 6 presents estimated PMPs after each of the adjustment steps, for different durations. The storm pattern is assumed to be a consecutive storm with 3 days duration in each case. The size of the first storm is 50% of the subsequent (second) storm. Design storm durations are taken to be 6 or 7 days, see Table 5.

3.2.4. Space–time PMP

The results of the estimation of PMP using the three alternative methods can be summarized as follows: Method (1) – statistical estimates: PMP is 382 mm for 24 h duration; Method (2) – generalized estimates from the Mekong River Basin, extrapolated to the Upper Ping River Basin: PMP is 348 mm, 3 day duration; Method (3) generalized estimates based on transposition from Tilda to the Upper Ping River Basin: PMP is 240 mm, 3 day duration.

From the above PMP depths and durations, four types of spatial and temporal PMP storms are constructed, as follows, and are used as inputs to the extreme flood model:

(1) Storm pattern I (PMP1): PMP depth is derived from generalized estimates from the Mekong River Basin, total depth is 522 mm, duration is 6 days (see Table 5), spatial pattern is isohyetal pattern as recommended by WMO (1986).
(2) Storm pattern II (PMP2): PMP depth is derived from generalized estimates based on transposition from Tilda, total depth is 363 mm, duration is 6 days (see Table 5), spatial pattern is the same as PMP1.
(3) Storm pattern III (PMP3): PMP depth and duration is the same as PMP2 but spatial pattern is the observed isohyetal pattern of Tilda.
(4) Storm pattern IV (PMP4): PMP depth is derived from statistical estimates, total depth is 573 mm, duration is 2 days, and spatial pattern is the same as PMP1.

Table 6
Estimated PMP for Upper Ping River Basin using transpositioning of severe typhoon "Tilda" and "Vae" for different durations.

Unit: mm

List of adjustments	Adjust factors	PMP for durations (h)					
		6	12	24	36	48	72
1. Observed extreme rainfall[a]	–	72	145	230	261	321	345
2. Distance inland	Decreased 20%	58	116	184	209	257	276
3. Barrier	Decreased 15%	49	99	156	177	218	235
4. Maximum humidity	Increased 3%	50	102	161	183	225	242

[a] Depth-area-duration from typhoon Tilda (September 21–25, 1964) and typhoon Vae (October 21–22, 1952)

3.3. Parameter estimation for catchment water balance model

The catchment water balance model requires three sets of input parameters relating to climate, soil and vegetation. Climatic inputs for the daily model are the observed time series of rainfall and potential evaporation. For soil parameters related to soil moisture capacity, the required parameters are (1) soil depth distribution, soil type, porosity and field capacity so as to determine the distribution of bucket capacities, (2) parameters related to storage–discharge relationship are determined from extensive analyses of observed recession curves. The parameters related to the distribution of bucket capacities are estimated from available maps of landforms, surveyed soil profile data related to each of the landform types, and other soil hydraulic properties for soils in this region. Jothityangkoon et al. (2001) described in detail how to estimate these parameters from available information.

3.3.1. Combination of linearity and non-linearity

The effect of non-linearity in subsurface runoff generation has been examined by Jothityangkoon and Sivapalan (2003) for a semi-arid catchment in Western Australia. They found that replacing linearity with non-linearity tended to increase the magnitude of peak flows. The effect of linearity and non-linearity was examined for a subcatchment of the Upper Ping River Basin through the simulation with the daily model. A comparison of the results in Fig. 2 reveals that the introduction of linearity or non-linearity in isolation does not give a good match to observed data. Linearity underestimates annual runoff, intra-annual variability and also under-estimate both the high flows and low flow parts of the flow duration curve whereas non-linearity overestimates the runoff and also high flow part of the flow duration curve. Combination of models involving linearity and nonlinearity (in parallel) in some proportion gives a better result, in this case, the proportion (α) was 1:1. Therefore, changing from semi-arid to tropical catchment

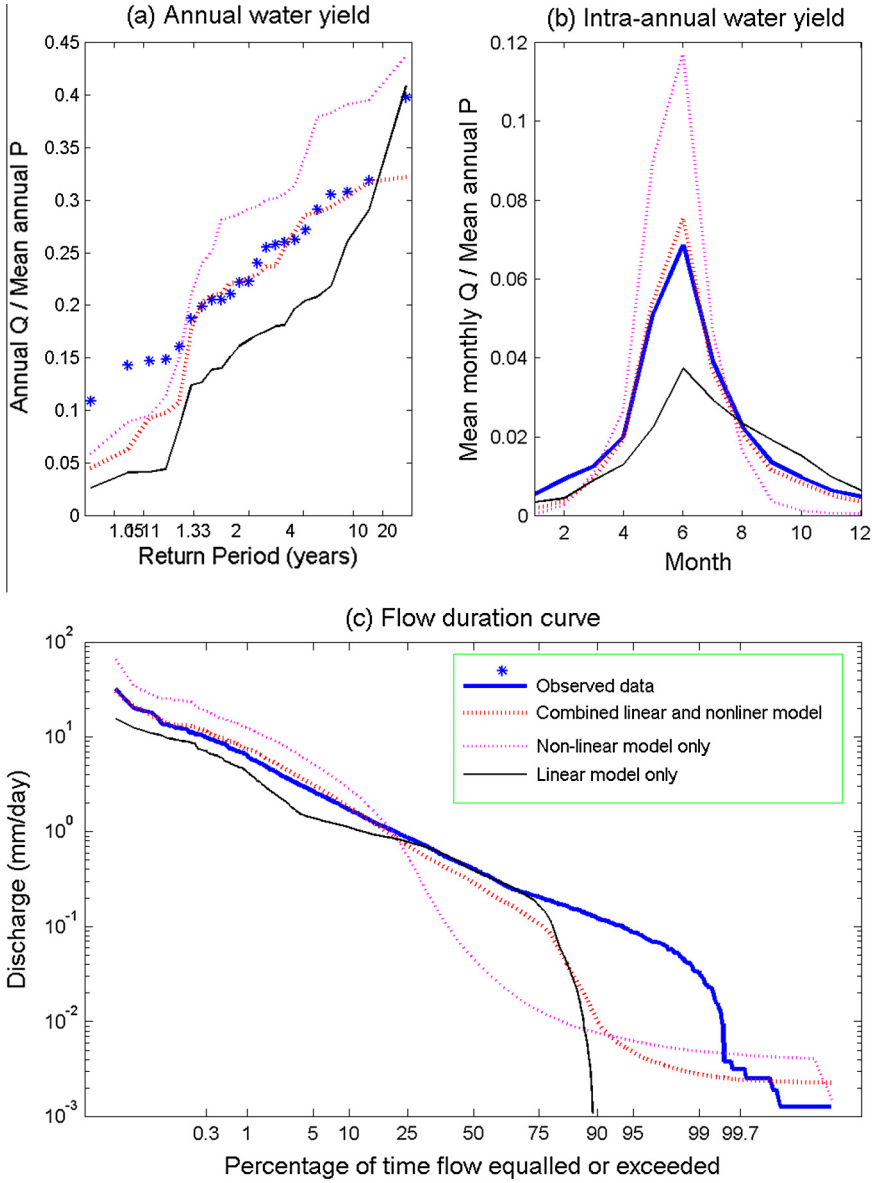

Fig. 2. Comparison of observed and simulated water yields between three cases of simulation: (1) combined linear and nonlinear storage–discharge relationship of subsurface runoff (2) non-linear storage–discharge relationship only (3) linear storage–discharge relationship only; (a) inter-annual water yield (mean yearly), (b) intra-annual water yield (mean monthly), (c) flow duration curve (based on daily flow) for station P.20 (sub-catchment No. 203, A = 1345 km^2).

Table 7
Estimated parameters for daily water balance model for four different subcatchments, where t_C is the catchment response time, a and b are the parameters of the storage–discharge model, α is the proportion of non-linear runoff generation, D is the average soil depth, ϕ is the average soil porosity, f_C is the soil's field capacity, M is the fraction of forest cover, k_V is the plant transpiration efficiency, i is the forest interception, λ is the proportion of the subsurface runoff percolating to the deep groundwater storage.

List of parameters	Cat – A Sub. Cat 182 11 km^2	Cat – B Sub. Cat 203 1346 km^2	Cat – C Sub. Cat 95 6359 km^2	Cat – D Sub. Cat 38 19,044 km^2
1. Model structure				
Number of subcatchments	1	6	162	179
Number of serial buckets in each subcatment	20	20	20	20
2. Storage–discharge relationship				
t_C (day)	500	500	500	500
a (mm$^{0.5}$ day$^{0.5}$)	100	20	20	20
b	0.5	0.5	0.5	0.5
α	0.1	0.5	0.5	0.5
3. Soil properties				
Measured D (m)	7.8	5.2	5.2	5.2
Adjusted D (m)	11.7	–	–	–
ϕ	0.4	0.4	0.4	0.4
f_C	0.16	0.16	0.16	0.16
4. Vegetation				
M	1.00	0.82–0.99	0.31–1.00	0.30–1.00
k_V	0.88	0.70	0.45–0.88	0.3–1.0
i (forest, %)	10	10	10	10
5. Deep groundwater				
λ	0.2	0.2	0.2	0.2
6. Stream routing				
Stream velocity (km/d)	50	50	50	50

requires one additional parameter to account for this proportion. The combined water yield (q_{sum}) from the catchment water balance is given by:

$$q_{sum} = \alpha(q^1_{total}) + (1-\alpha)(q^2_{total}) \quad (2)$$

where q_{total} from Eq. (A13) is separated to q^1_{total}: total water yield from non-linear runoff generation and q^2_{total}: total water yield from linear runoff generation and α is the proportion of non-linearity.

3.3.2. Parameters for all 220 subcatchments

The daily model configurations (multiple linear/non-linear buckets in series combined with a deep groundwater store and stream network routing) are the building blocks of a distributed model of the entire Upper Ping catchment. Based on topography and stream network and 15 basic sub-basins divided for water resources management and operated by the Department of Water Resources, the study catchment is divided into 220 sub-catchments. Each sub-catchment has its own input data and parameters with respect to climate, soils and vegetation. These parameters have already been estimated *a priori* for each sub-catchment. Simulated runoff from different sub-catchments is generated in parallel and is routed down the stream network. Table 7 shows the estimated parameters for four selected sub-catchments: Cat-A (11 km^2), Cat-B (1346 km^2), Cat-C (6359 km^2) and Cat-D (19,044 km^2) their locations presented in Fig. 1. Simulated results from these selected sub-catchments are compared to observed data.

Soil parameters for subsurface flow in the unsaturated zone and given in Eqs. (A16), (A17), (A18) using Δt = 1 h. Typical soil texture in the Upper Ping River Basin is sandy loam and clay so we use b = 4.9, $K_{hsat} = 3.47 \times 10^{-3}$ cm s^{-1} or 125 mm h^{-1} for sandy loam and b = 11.40, $K_{hsat} = 1.3 \times 10^{-4}$ cm s^{-1} or 4.7 mm h^{-1} for clay (Clapp and Hornberger, 1978). Based on analysis of stable isotope and permeability testing, Jundee (2004) found that potential groundwater recharge is about 12% of local annual rainfall. Converting this groundwater recharge to the proportion of subsurface runoff, λ in Eq. (A13) is assumed to be 0.2.

3.4. Parameter estimation for runoff routing model

Fig. 3a and b presented an example of the parameter estimation method based on surveyed channel cross-section and the observed rating curve at station PE.2 (19,044 km^2) or at the outlet of sub-catchment No.38. Given the channel cross-section in Fig. 3a and channel bed slope of 0.00057, a Manning coefficient (n_m = 0.045) is obtained first by fitting the simulated rating curve with the observed one, as shown in Fig. 3b, before converting to the effective Chezy coefficient of the main channel (C_m). As a first approximation, the Chezy coefficient in the flood plain is assumed to be the same as C_m of main channel. Simulated rating curve for the compound channel can be extrapolated from observed rating curve of the main channel (dash line in Fig. 3b). In the next step, the Chezy coefficient for the flood plain (C_f) including the effect of tree and/or building is estimated from previously known C_m. The distribution of trees and/or building in the flood plain were obtained from field surveys and satellite images from Google Earth and the range of representative values is presented in Table 8.

For each water level of over-bank flow, discharges for both main channel (Q_m) and floodplain section (Q_f) are estimated separately using C_m and C_f. To capture the effect of interaction between the flow in main channel and in the floodplain and the resulting boundary shear stress, these discharges are combined using the ϕ-index method. The empirical ϕ-indices were obtained from the laboratory experiments of Wormleaton and Merrett (1990), and are adopted in this study as well due to the lack of experimental evidence for the actual river reach, follow the previous work of Jothityangkoon and Sivapalan (2003).

Fig. 4b shows the estimated rating curves for three cases: (i) main channel only, (ii) compound channel by extrapolating the main channel curve and assuming no effect of trees and/or buildings, (iii) compound channel with the presence of trees and/or

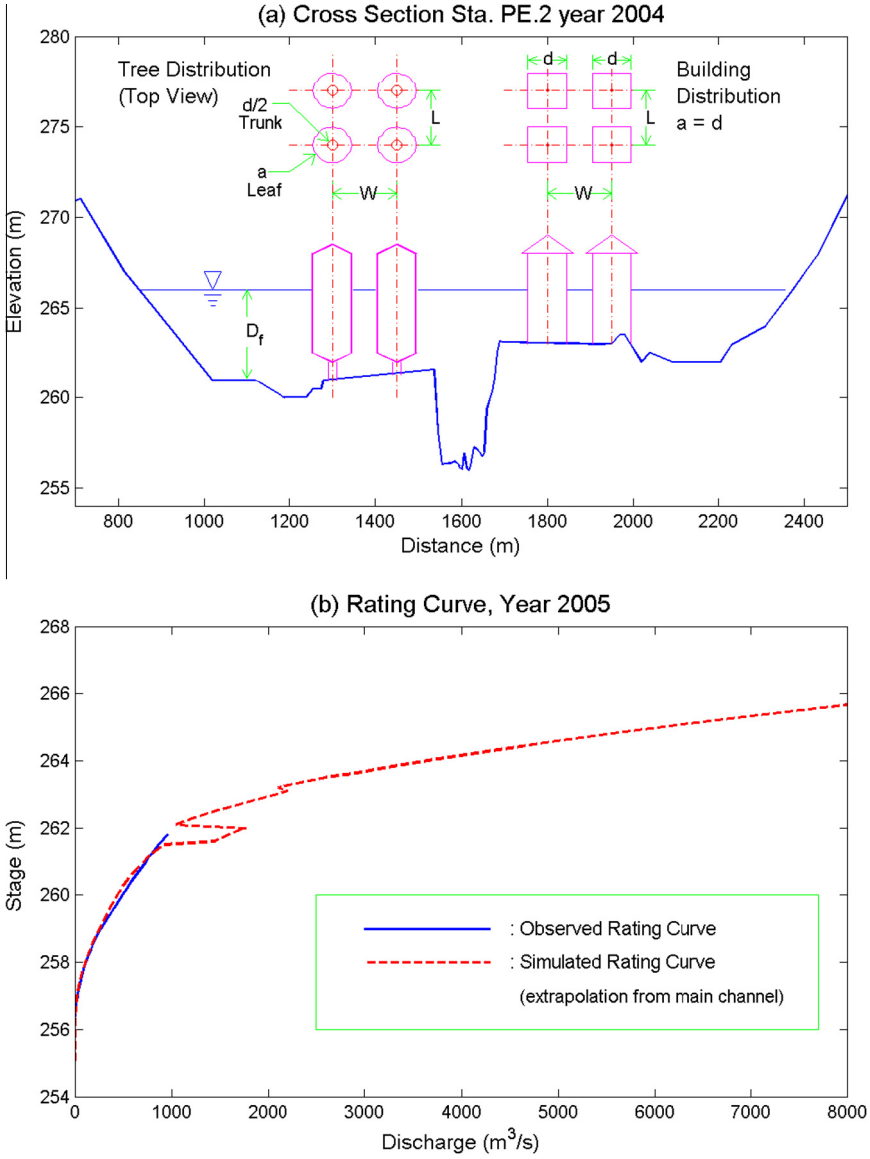

Fig. 3. Required hydraulic information at gauging station PE.2 or sub-catchment No. 38: (a) parameters of tree and building distribution on floodplain and the surveyed channel cross-section, (b) comparison of the measured and simulated rating curves with extrapolation from main channel to include floodplain geometry only, not including tree and building distribution.

Table 8
Parameters for trees and building distribution on floodplain, where L is the longitudinal interval of trees or buildings, W is the transverse interval of trees or buildings, a is the diameter of branch–leaf of trees or the length of buildings, d is the diameter of tree trunk or the width of buildings, β is the fraction of trees or buildings area in the floodplain.

Parameters	Unit	Range of values for	
		Trees	Building
L	m	5–12	8–15
W	m	5–12	10–20
a	m	4.5–11	8–12
d	m	0.2–0.5	8–12
β	–	0.05–1.0	0.1–0.7

Remarks: some subcatchments contain both trees and building, observed proportion of trees: building are varied between 0.4:0.6 and 0.8:0.2.

buildings. These stage–discharge curves in Fig. 4b are converted to storage–discharge curves using surveyed cross-section and measured channel length for the reach of subcatchment No. 38. The set of parameters k and m for main channel and compound channel are estimated by fitting power function to the calculated storage–discharge curves, as shown in Fig. 4c. The exponent m is about 0.8 when vegetation and/or building effects on the floodplain are ignored with ($n_f = n_m$) and it increases close to 1.0 with trees and/or building on the floodplain.

Table 9 presents an example of the estimated k and m parameters of the routing model at seven locations from the total of 34 reaches, corresponding to existing stream gauging stations. The storage–discharge curves of the compound channels are more linear ($m \approx 0.7$–1.1) than those of the main channel ($m \approx 0.4$–0.7). However, the compound channels of some reaches are still strongly non-linear (P.14). Checking these cross sections, it was found that the floodplains of these reaches are narrow as part of a rocky valley. To estimate k and m parameters for the remaining 186 river reaches, where local rating curve and cross-section information is not available, the storage–discharge curve is constructed from measured channel length and the cross-section and floodplain vegetation of neighboring subcatchments.

3.5. Application of rainfall–runoff model for PMF estimation

The estimation process consists of three main steps (Fig. 5):

(1) In the first step, based on long term water balance simulation, the antecedent soil-moisture storage in the catchment prior to receiving the PMP is estimated by using the catchment water balance model with a daily time step, running the simulation for a number of years up to the time of the selected event.
(2) In the second step, based on duration of storm event, PMP rainfall hyetograph is transformed into runoff hydrograph for each of the sub-catchments by running the catchment water balance model with an hourly time step.
(3) In the third step, the runoff generated in all the 220 sub-catchments in the previous step, is routed through the river network using the network routing model with a 10 min time step, and in this way the PMF is estimated at the catchment outlet.

3.6. Model validation

As mentioned in Jothityangkoon and Sivapalan (2003), the PMF is deemed as a very rare extreme event with probabilities in the range of about 10^{-3}–10^{-7}, extending far beyond what can be inferred from the relatively short available historical record. For this reason, estimates of the PMF can never be fully validated. The validation can be done through the application of the rainfall–runoff model only for some less-than-extreme events. However, the estimation of parameters should not just rely on mere calibration on less-than-extreme flood events. Instead, the mechanisms contributing to extreme

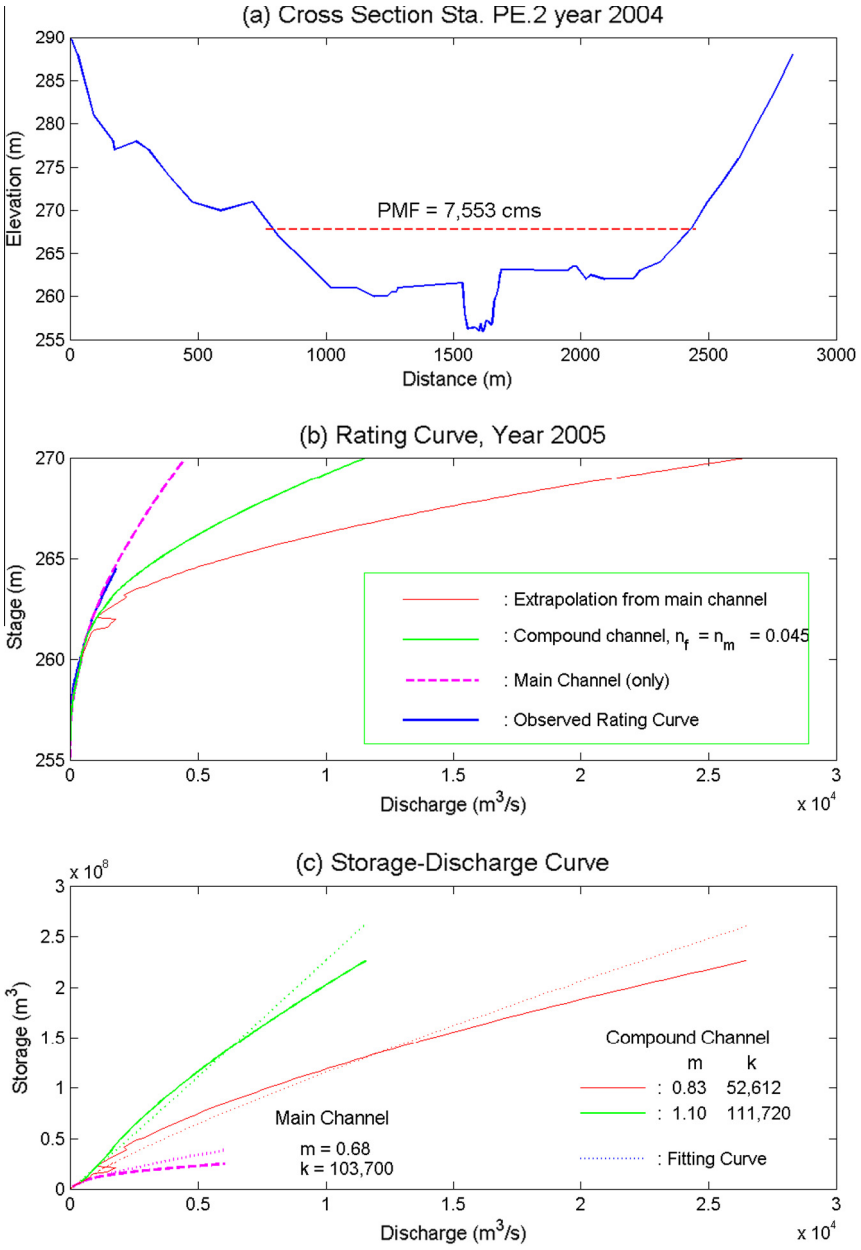

Fig. 4. An example of the estimated results for subcatchment No. 38 and stream gauge PE.2 of Upper Ping River (a) cross section,(b) estimated rating curve for compound channel, and extrapolation of main channel alone (c) estimated storage–discharge curves and parameters k and m for in-bank and over-bank flows. NB: n_m and n_f denote the Manning coefficient for the main channel and floodplain, respectively.

Table 9
Estimated parameters of runoff routing model from calculated storage–discharge curve, all gauge stations are in Chiang Mai province.

Site no.	Site name	Sub. no.	Area (km^2)	Main channel		Compound channel	
				m	*k*	*m*	*k*
P.1	Navarat bridge Mueang District	95	6350	0.43	395,370	1.08	12,319
P.14	Kang Oobluang Hod District	46	3836	0.68	36,997	0.72	28,567
P.19A	Ban Tasala Jomthong District	89	14,023	0.59	59,166	0.94	7699
P.20	Ban Chiengdao Chiang Dao District	203	1345	0.64	108,400	0.85	36,666
P.21	Ban Maerim Tai Maerim District	166	452	0.69	34,076	0.92	14,898
PE.2	Ban Kong Hin Hod District	38	18,932	0.68	103,700	1.10	111,720
60402	Huay Ban Chiang Dao District	182	12	0.71	3042	0.85	1776

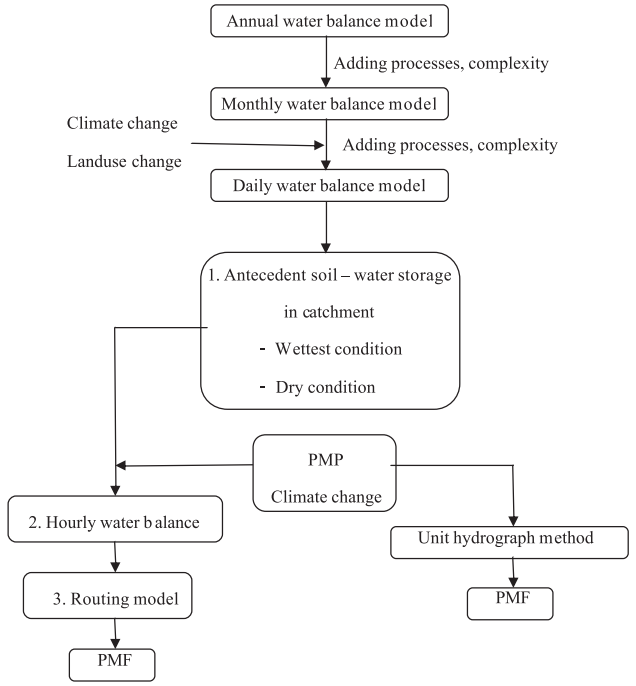

Fig. 5. Flow chart of procedure for extreme flood model development and estimation of PMF.

floods should be explored through sensitivity analyses combined with the model to estimate the uncertainty in the model predictions.

The catchment water balance model used in this study is developed with minimal calibration using procedures similar to those presented in in Jothityangkoon et al. (2001). Fig. 6 shows an example of the comparison between observed and simulated results for subcatchment No. 95 and stream gauge station P.1 ($A = 6359$ km^2). It shows that predictions by the model can generate a good match to the observed data. The catchment water balance model can be combined with the routing model to predict the short-term (hourly) response to a storm event. However, observed hourly discharge and rainfall in this catchment are not adequate to validate the combined model for individual events.

3.7. Approach to estimate uncertainty in the model prediction

To assess uncertainty in estimating extreme floods, the effects on model predictions under different scenarios and conditions are examined. The PMFs are estimated based on seven conditions to provide an assessment of uncertainty as follows:

(i) PMPs from different methods and spatial patterns,
(ii) antecedent catchment wetness, i.e. wet and dry,
(iii) PMFs from different locations and for different catchment sizes,
(iv) sensitivity study on the effects on increased rainfall,
(v) different routing parameters for the compound channel and for the extrapolation of the main channel,
(vi) sensitivity study on the effects of deforestation,
(vii) PMF estimates from previous models.

4. Results and discussion

4.1. PMFs due to different PMP Scenarios

PMFs were estimated for four different PMPs and it was found that the maximum PMF was obtained for PMP Type 4 at all locations with center at the center of the Upper Ping catchment (Table 10 condition (a)). The PMP Type 4 is derived by using statistical estimates with parameters determined from maximum rainfall data in USA, situated in the mid-latitudes. To adjust the atmospheric humidity to the maximum condition experienced in this region, a parameter called maximum common statistical variable (K_{max}) is required to be kept at a high value.

For the normal condition of a tropical climate close to equator, where the Upper Ping River Basin is located, atmospheric humidity is always high. If the high value of K_{max} based on rainfall data in USA is used for moisture adjustment to the maximum condition in tropical climate, an over-estimate of PMP can be expected, resulting in a high value of PMF. Estimated PMF from PMP Type 1 is more reliable than the PMFs estimated for the PMP types. Fig. 7 shows a comparison of the results of PMF hydrographs estimated for the four types of PMPs (from Fig. 9) for subcatchment 1 located at the Bhumipol Dam.

4.2. Different antecedent conditions

Using the same temporal and spatial patterns of PMPs, PMF estimates for the rainy season (September) are always higher than

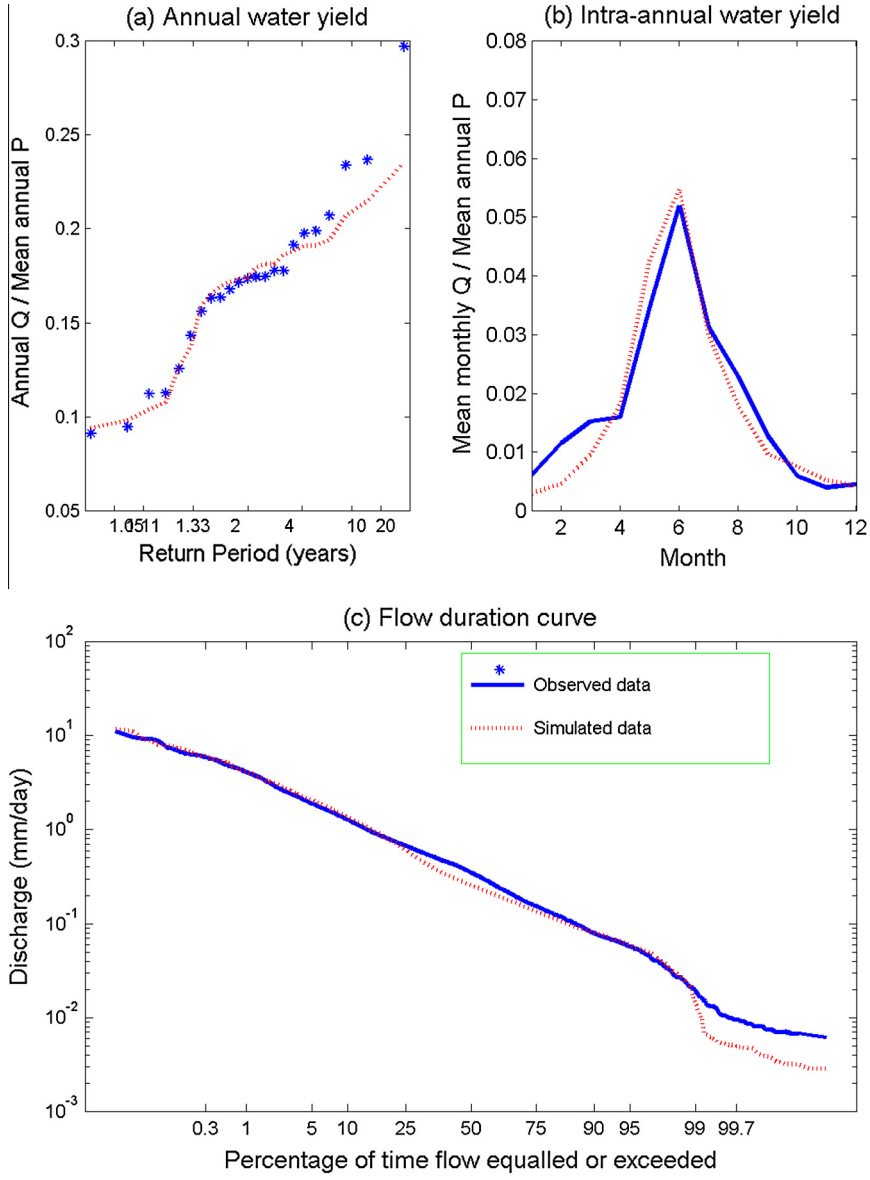

Fig. 6. Comparison of observed water yields from stream gauge P.1 and simulated water yields from daily water balance model for sub-catchment 95, $A = 6359$ km^2 (a) inter-annual variability, (b) intra-annual (mean monthly) variability, (c) flow duration curve (daily flows).

Table 10
Estimated PMFs for five different conditions at seven locations in the Upper Ping River Basin and from different PMPs: (a) typical four types of PMP (b) PMP1 with increasing of rainfall 5–15%,(c) using parameters extraporated from the main channel, (d) include the effects of deforestation.

Conditions	PMP type	PMF (m^3/s) from seven subcatchments Subcatchment numbers and its size (km^2)						
		1 26,202	38 19,043	89 13,990	95 6359	203 1345	204 202	182 11
(a) PMP in the wettest condition	PMP 1	6311	7553	6518	3310	571	92	4.2
	PMP 2	3455	3618	3565	2207	288	52	2.3
	PMP 3	2207	2607	1850	727	82	21	0.7
	PMP 4	8693	11,998	11,697	6456	1,350	309	17.1
(b) PMP in summer	PMP 4 (dry)	2434	3869	3924	1803	29	3	0.03
(c) Rain increase 5–15% by La Niña	PMP 1 + 5%	6784	8154	7080	3576	620	105	4.6
	PMP 1 + 10%	7262	8778	7610	3812	669	114	5.7
	PMP 1 + 15%	7755	9408	8176	4066	717	122	6.0
(d) Using m, k from main channel	PMP 1	16,121	14,663	11,677	4766	579	96	4.2
(e) Deforestration 10%	PMP 1	6507	7798	6726	3399	605	103	5.3
Deforestration 20%	PMP 1	6703	8042	6954	3497	632	105	5.4
Deforestration 30%	PMP 1	6894	8267	7113	3550	671	115	6.4

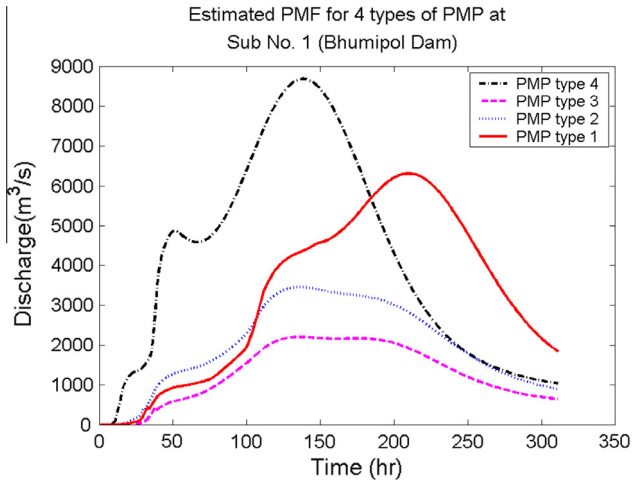

Fig. 7. Comparison of PMF hydrograph derived from four types of PMP at sub-catchments No.1, upstream of Bhumipol dam.

for the summer (May) due to the higher antecedent wetness (Table 10 condition (a) and (b) PMP 4).

4.3. PMFs from different locations

The estimated PMFs for subcatchment 1 or the Bhumipol Dam are always lower than the PMFs at some upstream subcatchments (i.e. 38 and 89 in Table 10) and Fig. 8. The reason of this behavior is the attenuation of the hydrograph due to the effect of routing in channel storages. The center of the isohyetal pattern of PMP is in the middle of the Bhumipol Dam catchment. This causes a smaller contribution of runoff from subcatchments close to the dam, and allows the shape of the outflow hydrograph to be dominated by the attenuation effect of channel routing.

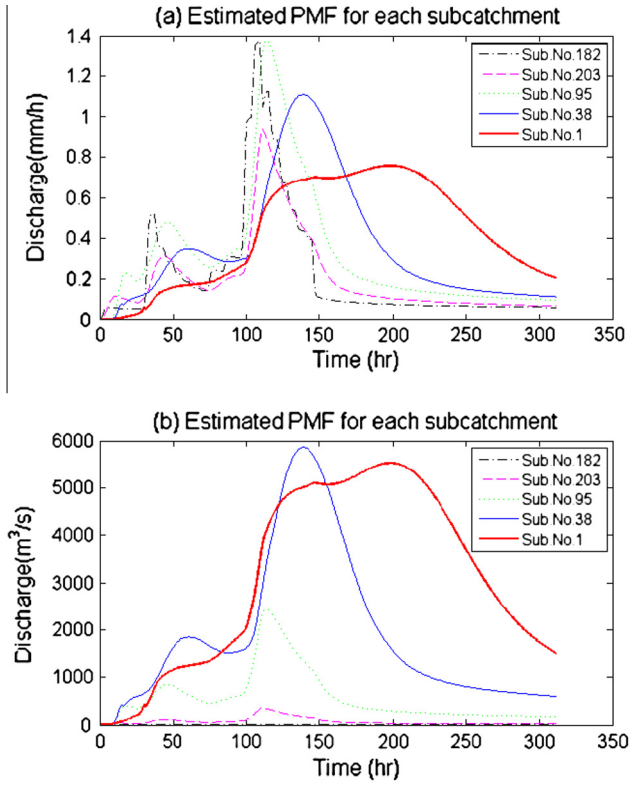

Fig. 8. Estimated PMF hydrograph from five different sub-catchments based on PMP 1 (a) unit of discharge in mm/h (b) unit of discharge in m^3/s.

4.4. PMF and climate change

Kripalani and Kulkarni (1997) investigated the years of El Niño (La Niña) events above- and below-normal epochal behavior of rainfall within the Asian monsoon region. They found that the differences between the means of the average standardized rainfall for the above- and below-normal epochs are significant at the 5% level for Thailand, Malaysia, Singapore and Brunei. The majority of the La Niña related floods have occurred during above normal epochs, e.g., Thailand (1938, 1970). The epochs tend to last for about one decade over the equatorial oceanic regions and about three decades over continental regions. To test the effects of such natural climate variability, the increase of PMP caused by La Niña is used as input to the extreme flood model to generate the corresponding PMF. Table 10 condition (c) shows that if PMP1 is increased by 5%, 10% and 15%, the PMF at Bhumipol Dam will increased from 6311 m^3/s to 6784, 7262 and 7755 m^3/s or increase by 7.5%, 15.1% and 22.9%, respectively.

4.5. PMF and floodplain inundation

The routing parameters estimated from compound channels always give a lower PMF estimate (Table 10 condition (a)), compared to PMFs estimated from routing parameters estimated from extrapolation of the main channel (Table 10 condition (d)). This result shows that the floodplain resistance when the dominant runoff process changes from in-bank flow to over-bank flow reduces the magnitude of the PMF. The estimated PMF at sub-catchment No. 38 (19,043 km^2) in Table 10 condition (a) shows that the estimated PMF from PMP Type 1 during the rainy season is 7553 m^3/s. This estimated PMF can be converted to water level in the channel using the estimated rating curve, as shown in Fig. 4a. It can be seen that the estimated PMF is very large, about four times the observed maximum flood of 1580 m^3/s measured at the same location, gauging station PE.2. The simulated inundation width on the floodplain extends to a distance of about 1700 m across both sides of the compound channel cross section. The water level for this flood could be 3.8 m above the current highest stage (264 m MSL) in the surveyed channel cross section. In-bank flow remains the dominant runoff process only if the discharge stays below 1790 m^3/s, as shown in Fig. 4a. It is clear from this that over-bank flow and floodplain inundation will be the dominant runoff process under such extreme flow condition.

4.6. PMF and land-use change

A consequence of the decrease of forest area within the Upper Ping River Basin by 10%, 20% and 30%, is found to increase the PMF at sub-catchment 1 or Bhumipol Dam (from 6311 m^3/s in case of PMP1) to 6507, 6703 and 6894 m^3/s or by 3.1%, 6.2% and 9.2%, respectively, see Table 10 condition (e).

4.7. PMF estimates from previous methods

The design extreme flood for the Upper Ping River Basin at Bhumipol Dam has been reviewed by the unit hydrograph method, to investigate the effect of physical and land-use changes. The unit hydrograph method uses time invariance, therefore an updated unit hydrograph is required and is estimated here based on present stream flow hydrographs and current rainfall–runoff relationships, which can capture the effects of all physical changes in the catchment that have happened in the last few decades. The main problem is that the old stream gauge was abandoned since the dam was

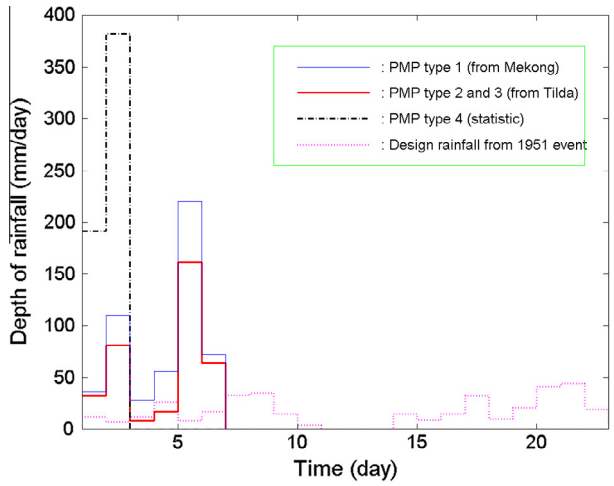

Fig. 9. Hytegraph of four different design rainfall patterns: PMP1 from Mekong, PMP2&3 from Tilda, PMP4 from statistic estimates and design rainfall from 1951 event.

built. It is not possible to have the present streamflow hydrograph at the same location as that of the design period. The synthetic unit hydrograph based on the study of Taesombut (2001) has been used as a substitute. This study utilizes all available rainfall–runoff data at different locations and different sizes of subcatchments within the basin to estimate synthetic unit hydrographs and dividing the Upper Ping river basin into 22 subcatchments to represent its stream network. Excess rainfall is estimated by ϕ-index method. Discrete convolution method is used to convert the excess rainfall to the outflow hydrograph of each subcatchment. Finally, these outflow hydrographs are routed though stream network using the Muskingkum routing method. Using the old design rainfall as input (Fig. 9), the corresponding extreme flood at the dam site is estimated to be 7168 m^3/s, which is higher than the original design flood (6000 m^3/s). Using this model to convert PMP1 to PMF, the corresponding extreme flood will be 8749 m^3/s, as shown in Table 11.

For preliminary estimates, envelope curves based on historical flow data are often used to check the validation of the final design values. The Economic and Social Commission for Asia and the Far East (ECAFE) secretariat (currently changed to the United Nations Economic and Social Commission for Asia and the Pacific (ESCAP) has published a series of envelop curves for maximum floods for the monsoon areas in Southeast Asia and the Far East. The ECAFE envelop curve for Southeast Asia shows that maximum floods for the Upper Ping River Basin is 0.305 $m^3/s/km^2$ or 8050 m^3/s. An envelope curve for Thailand prepared by the Royal Irrigation Department (RID) provides the value of 0.277 $m^3/s/km^2$ or 7310 m^3/s. (ECI Engineering Consultants Inc., 1969). North America and many other countries prefer to use the PMF as a basis for design flood criteria. However, some countries in Europe prefer to use flood frequency analysis thanks to the availability of long records of historical flow data. Zielinski (2011) concludes that the preference of using of a specific design flood depends on individual and group safety and the criteria should be selected from the perspective of general, national safety and social desires.

4.8. Uncertainty of PMP and PMF estimates

Estimated results from Section 4.4 show that PMP is a main critical parameter influential to uncertainty of PMF estimates. To deeply investigate the uncertainty analysis in PMP, deterministic envelop curve (depth-duration-area curve) used in Section 3.2.2 may be modified to probabilistic regional envelop curves proposed by Castellarin (2007) and Castellarin et al. (2009). Castellarin (2007) suggest that the reliability of design flood estimates depends on selected correlation formula or plotting position of observed maximum rainfall. If the probabilistic regional envelop curves (design flood depending on catchment area alone) are extended to multivariate regional envelopes (design flood depending on climatic and geomorphologic characteristics of basin), the accuracy of design flood estimates will be increased (Castellarin et al., 2007). Viglione et al. (2012) assess the reliability of rainfall quantiles for large return period with two methods, the depth-duration envelop curves and extreme rainfall quantiles obtained from stochastic rainfall generators. They found that estimated reliable point rainfall quantiles with high return period can be achieved by the use of combined regional and local methods.

5. Conclusions

By using distributed rainfall–runoff model, this paper has demonstrated that climate and land use changes can cause significant changes in the magnitude of extreme floods. The distributed rainfall–runoff model, consisting of a subcatchment runoff generation model and a distributed runoff routing model in channel networks, is used to transform PMP to PMF in the Upper Ping catchment at the location of Bhumipol Dam. To apply of this model (developed originally for a semi-arid catchment) to a tropical catchment required the addition of two more physical parameters. These parameters are weighting factor to account for linearity and nonlinearity of subsurface runoff generation process, and combination of distributions of trees and buildings on the floodplain. However, the model has not considered infiltration excess runoff which could in runoff generation play important role if the proportion of land use put to agricultural and urban uses is increased leading to compaction of the soil surface.

The most reasonable PMP chosen to fit the Upper Ping catchment has 3 day duration and 348 mm depth, estimated by the method of generalized estimation from the Mekong River Basin. This PMP is used to construct PMP storm with 6 day duration and a total 552 mm depth (PMP Type 1), distributed over the whole catchment, which is divided into 220 subcatchments. The PMP estimation method should be extended in the future from the deterministic approach used in this study to more stochastic approaches to estimate the uncertainty in the PMP estimates, similar to the work of Viglione et al. (2012).

The simulation results from the proposed extreme flood model show that estimated PMF values at the dam site is 6311 m^3/s which higher than design maximum flood (6000 m^3/s) from a flood study report carried out in 1955. By using original design method based on the lumped unit hydrograph model with the current shape of unit hydrograph, effective rainfall of previous design rainfall is converted to design maximum flood. The results still show

Table 11
Comparison of estimated PMF between three methods and four types of design extreme rainfall.

Methods	Estimated extreme flood or PMF (m^3/s)				
	Old design rainfall	PMP1	PMP2	PMP3	PMP4
1. Single unit hydrograph	6000	–	–	–	–
2. Synthetic unit hydrograph for 22 Sub. + routing model	7168	8749	4716	1993	13,670
3. Proposed extreme flood model	–	6311	3455	2207	8693

that maximum design flood at the dam could increase from 6000 to 7168 m^3/s or by 15%. Land use change during past 50 years is the main cause of this increase. If the PMP is transformed to PMF using the unit hydrograph model with current shape, estimated PMF will be increased to 8749 m^3/s. These simulated results also indicate that estimated PMF can be over-estimates if the effects of floodplain inundation, vegetation and building cover on floodplains are not included, similar to results obtained by Jothityangkoon and Sivapalan (2003). To gain more confidence to the PMF estimates, further work should be focused on validation of the assumption of over-bank flow processes such as, interaction between the flow in main channel and in the floodplain, the real Chezy coefficient for the floodplain including the effect of trees and/or buildings.

The testing of extreme flood processes in the mean of uncertainty analysis of model estimation is performed to determine the critical parameters and processes influential to uncertainty of extreme flood prediction. The estimated PMF is the most sensitive to input PMP, deforestation, catchment wetness, and floodplain inundation effect. For example, a 5% increase in PMP depth cause 7.5% increase in PMF (from 6311 to 6784 m^3/s), 10%, 20% and 30% of deforestation result PMF increased by 3.1%, 6.2% and 9.2% respectively. Changing the antecedent soil moisture condition from wet to dry will contribute to a decrease of the PMF from 8693 m^3/s in the rainy season to 2434 m^3/s in summer (72%). Considering over-bank flow involving compound channel (using compound channel parameter m close to 1 in Table 9), PMF will be decreased to 6311 m^3/s compared to 16,121 m^3/s (using main channel parameters m close to 0.6 in Table 9). More research should be carried out to investigate the impact of these parameters and the processes that could potentially occur under extreme conditions. That will lead not only to reasonable reduction of estimated PMFs but also a reduction of the uncertainty of PMF estimates.

Based on this investigation, the operation of dam safety and storage water management should be treated with caution, particularly during the monsoon season. The main priority of the dam to store water for hydropower and irrigation for the following summer may cause inadequate empty space in the reservoir of the dam. This empty storage is required for attenuation of inflow flood hydrograph through reservoir routing and flood protection of the downstream area. On the other hand, subsequent development in the floodplain downstream of the dam has reduced the safe release during severe flooding condition. During September–October 2011, heavy rainfall in the Ping River Basin and poor management of water release from this large dam was blamed for the severe flood that occurred in the central part of Thailand and in Bangkok.

Acknowledgements

The authors are grateful to the Electricity Generating Authority of Thailand (EGAT) for financial and technical support for this project. Grateful acknowledgements are given to Thai Meteorological Department, Royal Irrigation Department, Department of Water Resources, Department of Groundwater Resources, and the Land Development Department for providing field data. Special thanks go to Assoc. Prof. Amnat Apichatvallop for useful comments.

Appendix A.

A.1. Catchment water balance model

The catchment water balance (rainfall–runoff) model used in this study is an adaptation of a sub-catchment based distributed water balance model developed by Jothityangkoon et al. (2001). The difference between the previous work and the present one is the change of the target catchment from a large semi-arid catchment to an even larger tropical catchment. The proposed model is a distributed one, with its building blocks being a large number of sub-catchments which are organized around the river network. This section describes the runoff generation component at the subcatchment scale, whereas the routing of the runoff within the river network is described in the next section.

To formulate a water balance model of appropriate complexity, the systematic downward approach of Klemes (1983) was adopted (see also Sivapalan et al., 2003), where the model has been developed in progressive steps focused on reproducing runoff variability at the annual, monthly and daily timescales and model simulations in each case are compared against signatures of runoff variability estimated at each timescale. All models operate on a daily time step. The annual water balance model is the first model step and consisted of a simple partitioning of rainfall into evaporation and saturation excess runoff, and the focus is on reproducing the inter-annual variability only. The model required only three parameters: soil depth, mean porosity and the fraction of rainfall that is intercepted on vegetation canopy (i.e., interception loss). Of course, this model was found to be inadequate to explain the intra-annual (within-year, e.g., mean seasonal) variability of runoff.

The monthly water balance model represents the step in the model progression. It incorporated additional processes, e.g., the generation of subsurface runoff through the use of a linear storage–discharge relationship, and the partitioning of evapotranspiration into bare soil evaporation and transpiration. Inclusion of these additional processes involved addition of new parameters; four soil and topographic parameters and two vegetation parameters. The signature of interest here is the regime curve, i.e., mean monthly variation of runoff. The final step in the evolution of model complexity was the daily model, with the signature of interest being the flow duration curve, and of course the complete daily runoff hydrograph. Additional process complexities considered in this third type of model include a non-linear storage–discharge relationship, multiple buckets in series to capture the variability of soil depths within the catchment, and deep groundwater storage. In the rest of this section, we present the details of the daily water balance model at the level of a single bucket (a multiple bucket model will involve the parallel operation of these buckets belonging to each subcatchment). The water balance equation for the single bucket model with daily input data is given by:

$$\frac{ds(t)}{dt} = i(t) - q_{ss}(t) - q_{se}(t) - e_b(t) - e_v(t) \tag{A1}$$

where $s(t)$ is the depth of soil moisture storage, $i(t)$ is the rainfall intensity, $q_{ss}(t)$ is subsurface flow, $q_{se}(t)$ is the saturation excess runoff, e_b is bare soil evaporation and e_v is transpiration.

A.1.1. Subsurface runoff

$$q_{ss} = \frac{s - s_f}{t_c} \quad \text{if } s > s_f \tag{A2a}$$

$$q_{ss} = 0 \quad \text{if } s < s_f \tag{A2b}$$

where s_f is the soil-moisture storage at field capacity, and t_c is a catchment response time of subsurface flow. The threshold storage, s_f is assumed to be $s_f = f_c D$, where f_c is the soil's field capacity and D is the average soil depth. The response time t_c is estimated by applying Darcy's law to an idealized, triangular representation of the groundwater aquifer within a planar hillslope, assuming that the hydraulic gradient can be approximated by the slope of the ground surface. This gives:

$$t_c = \frac{L\phi}{2K_s \tan\beta} \tag{A3}$$

where ϕ is average soil porosity, L is average hillslope length, tan β is average ground surface slope, and K_s is the average saturated hydraulic conductivity.

For nonlinear storage discharge relationship, the single parameter t_c is replaced by the following nonlinear relationship with two parameters a and b:

$$q_{ss} = \left[\frac{s - s_f}{a}\right]^{\frac{1}{b}} \quad \text{if } s > s_f \tag{A4a}$$

$$q_{ss} = 0 \quad \text{if } s < s_f \tag{A4b}$$

where parameter a and b can be estimated directly from recession curve analysis using an iterative least squares fitting method (Wittenberg, 1994).

A.1.2. Saturation excess runoff rate

$$q_{se} = s - S_b \quad \text{if } s > S_b \tag{A5a}$$

$$q_{se} = 0 \quad \text{if } s < S_b \tag{A5b}$$

where S_b, is the bucket's soil moisture storage capacity, given by $S_b = D\phi$ and Δt is the time step.

A.1.3. Bare soil evaporation rate

$$e_b = \frac{s}{t_e} \tag{A6}$$

$$t_e = \frac{S_b}{(1-M)e_p} \tag{A7}$$

where t_e is a characteristic time scale associated with bare soil evaporation, e_p is the potential evaporation rate, and M is the fraction of forest vegetation cover ($0 < M < 1$).

A.1.4. Transpiration rate

$$e_V = Mk_V e_p \quad \text{if } s > s_f \tag{A8}$$

$$e_V = \frac{s}{t_g} \quad \text{if } s < s_f \tag{A9}$$

$$t_g = \frac{s_f}{Mk_V e_p} \tag{A10}$$

where t_g is a characteristic time scale associated with transpiration and, following Eagleson (1978), k_V is a plant transpiration efficiency (generally set equal to 1).

A.1.5. Deep groundwater runoff

An underlying deep groundwater store was added to the above soil moisture store to account for baseflow. The water balance equation for the deep groundwater store is given by

$$\frac{ds_g(t)}{dt} = \lambda q_{ss}(t) - q_{sg}(t) \tag{A11}$$

$$\text{with} \qquad q_{sg}(t) = \left[\frac{s_g}{a}\right]^{\frac{1}{b}} \tag{A12}$$

$$\text{and} \qquad q_{total} = (1-\lambda)q_{ss} + q_{sg} + q_{se} \tag{A13}$$

where $s_g(t)$ is the volume of deep groundwater storage, q_{ss} as before is the subsurface runoff rate, λ is the proportion of the subsurface runoff percolating to the deep groundwater storage, q_{sg} is groundwater runoff and q_{total} is total water yield from the catchment.

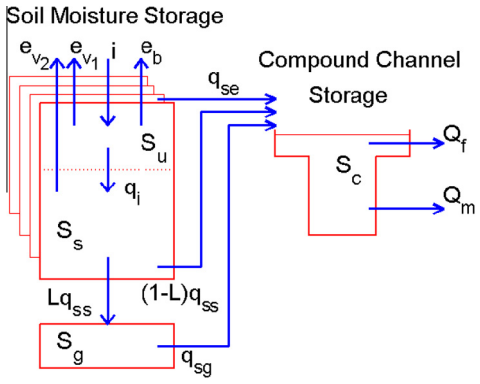

Fig. A1. Schematic of the combination of hillslope water balance model based on hourly time step and runoff routing model, where s_s is the saturated storage, s_u is the unsaturated storage, s_g is the deep groundwater storage, s_c is the channel storage, e_{v1} and e_{v2} are the potential transpiration rate, q_i is the outflow rate from s_u to s_s, q_{ss} is the subsurface runoff rate, $L = \lambda$ is the proportion of the subsurface runoff percolating to the deep groundwater storage, q_{se} is the saturation excess runoff, q_{sg} is the groundwater runoff, Q_m is the main channel discharge and Q_f is the floodplain discharge.

For runoff simulations during extreme flood events, the water balance model was extended to an hourly time step by adding one more process, a delay mechanism in the unsaturated zone. The volume of lumped soil moisture storage in (A1) is separated into a saturated storage (s_s) and an unsaturated storage (s_u). These two storage zones are connected by an internal flow (to account for recharge or capillary rise). A schematic of the inflow and outflow rates from the different storages are presented in Fig. A1. The water balance equations for s_u and s_s are given by:

$$\frac{ds_u(t)}{dt} = i(t) - e_b(t) - e_{v1}(t) - q_i(t) - q_{se}(t) \tag{A14}$$

$$\frac{ds_s(t)}{dt} = q_i(t) - e_{v2}(t) - q_{ss}(t) \tag{A15}$$

where $q_i(t)$ is the outflow rate from s_u to s_s. In this case, because this model is only applied during or immediately after storm events, e_{v1} and e_{v2} are formulated such that $e_{v1} + e_{v2}$ is equal to the potential transpiration rate $k_v \cdot M \cdot e_p$. When the unsaturated zone cannot deliver evaporation at the potential rate, water is extracted from the saturated store. Internal flow rate q_i can be expressed as a function of hydraulic conductivity, K_h, and the hydraulic gradient, and K_h can be approximated as a function of saturated hydraulic conductivity, K_{hsat}, and the degree of saturation, S, $S = s_u/s_{ub}$, Δt is the time step:

$$q_i = K_h\left(1 + \frac{i\Delta t}{s_{ub}}\right) \tag{A16}$$

$$K_h = K_{hsat}S^c \tag{A17}$$

$$c = 2b + 3 \tag{A18}$$

A.2. Runoff routing model

Runoff produces from each of the sub-catchments, as modeled above, flows to the nearest stream channel and is then routed down the channel network. The network routing model is based on a conceptualization of each channel link in the network operating as a nonlinear reservoir, similar to the RORB model (Laurenson and Mein, 1988). The response of each channel reach is modeled by

solving the water balance equation $ds_c/dt = I(t) - Q(t)$ coupled with a non-linear storage (s_c) to discharge (Q) relationship expressed as a power function $s_c = kQ^m$ where k and m are model parameters, $I(t)$ represents the summation of input flows, both lateral inflow from the adjacent sub-catchment and flows from the upstream channel reaches (in the case of higher order reaches). The parameters k and m are estimated separately for each of the stream reaches. These parameters may become substantially different when the physical characteristics of river flow transition from normal floods to extreme floods, especially in the case of a transition from in-bank to over-bank flow (Wormleaton and Merrett, 1990; Jothityangkoon and Sivapalan, 2003).

For estimation of k and m in actual rivers, recorded stage–discharge curves (known as rating curves) are normally used, combined with available information on the geometry of main channel, cross section and length of the river reach. However, recorded rating curves may not include the effect of over-bank flows experienced during extreme floods because of the rarity of these extreme events and the difficulty of field measurements during these conditions. For the estimation of the rating curves beyond recorded data, river cross section is treated as a compound channel and subdivided into a main channel and floodplain sections. Discharge from each section is estimated separately. In the case of the main channel, the empirical storage–discharge curve is used directly. In the case of floodplain, the simulated storage–discharge curve is estimated by using a methodology developed by Tamai (1992a,b), considering of the effect of vegetation and other bulk flow resistances that may be present in the flood plain, the effects of which are expressed in terms of an equivalent Chezy coefficient. Discharge from both sections are combined to construct the rating curve and a storage–discharge curve by including the effect of momentum transfer between the main channel and floodplain (Wormleaton and Merrett, 1990). Details of this procedure are described by Jothityangkoon and Sivapalan (2003). In large catchments typical of Asian countries, there are not only forests or orchards occurring in the floodplain, but houses and other buildings as a part of human settlement. The flow resistance in the floodplain due to the size and spacing of houses and buildings are considered in the same manner as they are estimated in the case of floodplain vegetation (e.g., Tamai, 1992a,b).

References

Brakenridge, G.R., 2013. Global Active Archive of Large Flood Events. Dartmount Flood Observatory, University of Colorado. <http://floodobservatory.colorado.edu/Archives/index.html> (accessed 21.01.13).

Bureau of Reclamation, 1955. Report on Yanhee Project Thailand, for Power, Irrigation, Flood Control & Navigation, Appendix I: Inflow Design Flood, Denver Colorado.

Bureau of Reclamation, 1990. Flood Hydrograph and Routing System (FHAR), Computer Model Version 4.14, Technical Service Center, Denver, CO.

Castellarin, A., 2007. Probabilistic envelop curves for design flood estimation at ungauged sites. Water Resour. Res. 43 (4). http://dx.doi.org/10.1029/2005WR004384.

Castellarin, A., Merz, R., Blöschl, G., 2009. Probabilistic envelop curves for extreme rainfall events. J. Hydrol. 378, 263–271.

Castellarin, A., Vogal, R.M., Matalas, N.C., 2007. Multivariate probabilistic regional envelopes of extreme floods. J. Hydrol. 336, 376–390.

Chao, B.F., Wu, Y.H., Li, Y.S., 2008. Impact of artificial reservoir water impoundment on global sea level. Science 320 (5), 212–214. http://dx.doi.org/10.1126/science.1154580.

Clapp, R.B., Hornberger, G.M., 1978. Empirical equations for some soil hydraulic properties. Water Resour. Res. 14, 601–604.

Croke, B.F.W., Merrit, W.S., Jakeman, A.J., 2004. A dynamic model for predicting hydrologic response to land cover changes in gauged catchment. J. Hydrol. 291, 115–131.

Daojiang, Z., Jinshang, Z., 1984. Recent developments of the probable maximum precipitation (PMP) estimation in China. J. Hydrol. 68, 285–293.

Eagleson, P.S., 1978. Climate soil, and vegetation 1. Introduction to water balance dynamics. Water Resour. Res. 14 (5), 705–712.

ECI Engineering Consultants INC., 1969. Nan River Multipurpose Project: Nan River Basin Hydrometeorological Report, Prepared for Royal Irrigation Department.

Electricity Generating Authority of Thailand, 1988. Technical Data of Dams, Appurtenant Structures and Hydro Power Stations of EGAT, Report No. 31210–3101, Hydro Power Construction Department.

England Jr., J.F., Julien, P.Y., Velleux, M.L., Smith, J.A., 2005. Distributed modeling of extreme floods on large watersheds. Proceedings of World Water and Environmental Resources Congress 2005, ASCE.

Graham, W.J., 2000. Should dams be modified for the probable maximum flood? J. Am. Water Resour. As. 36 (5), 953–963.

Hansen, E.M., 1987. Probable maximum precipitation for design floods in the United States. J. Hydrol. 96, 267–278.

Hansen, E.M., Schreiner, L.C., Miller, J.F., 1982. Application of probable maximum precipitation estimates. United States east of the 105th Meridian, Hydrometeorol. Rep. No. 52, Natl. Weather Serv., US Dep. Commer., Silver Spring, Md., 228 pp.

Harris, J., Brunner, G., 2011. Approximating the probability of the probable maximum flood. Proceedings of the 2011 World Environmental and Water Resources Congress, ASCE.

Hershfield, D.M., 1961. Estimating the probable maximum precipitation. J. Hydraul. Div. ASCE 87 (HY5), 99–116.

Institution of Engineers, 2001. Australian Rainfall and Runoff, Volume One: A Guide to Flood Estimation, Australia.

Institute of Hydrology, 1999. Flood Estimation Handbook (FEH), Procedures for Flood Frequency Estimation, Wallingford, Oxfordshire, United Kingdom.

Jarrett, R.D., Tomlinson, E.M., 2000. Regional interdisciplinary paleoflood approach to assess extreme flood potential. Water Resour. Res. 36 (10), 2957–2984.

Jothityangkoon, C., Sivapalan, M., 2003. Towards estimation of extreme floods: examination of the roles of runoff process changes and floodplain flows. J. Hydrol. 281, 206–229.

Jothityangkoon, C., Sivapalan, M., Farmer, D.L., 2001. Process controls of water balance variability in a large semi-arid catchment: downward approach to hydrological model development. J. Hydrol. 254, 174–198.

Jundee, E., 2004. Hydrogeology of the Groundwater Resource at the Mae Hae Royal Project Development Center, Mae Chaem District, Chiang Mai Province, Master Thesis, Chiang Mai University, Thailand.

Klemes, V., 1983. Conceptualisation and scale in hydrology. J. Hydrol. 65, 1–23.

Kripalani, R.H., Kulkarni, A., 1997. Rainfall variability over south-east Asia connections with Indian Monsoon and ENSO extremes: new perspective. Int. J. Climatol. 17, 1155–1168.

Kuchment, L.S., Gelfan, A.N., 2011. Assessment of extreme flood characteristics based on a dynamic-stochastic model of runoff generation and the probable maximum discharge. J. Flood Risk Manage. 4, 115–127.

Laurenson, E.M., Mein, R.G., 1988. RORB-Version 4 Runoff routing Program – User Manual, Department of Civil Engineering, Monash University, p. 186.

Laurenson, E.M., Mein, R.G., Nathan, R.J., 2006. RORB-Version 5 Runoff Routing Program – User Manual. Monash University, Department of Civil Engineering.

Mein, R.G., Laurenson, E.M., McMahon, T.A., 1974. Simple nonlinear model for flood estimation. J. Hydraul. Div. ASCE 100 (HY11), 1507–1518.

Ohara, N., Kavvas, M.L., Kure, S., Chen, Z.Q., Jang, S., Tan, E., 2011. Physically based estimation of maximum precipitation over American river watershed, California. J. Hydrol. Eng. 16 (4), 351–361.

Pinter, N., Ickes, B.S., Wlosinski, J.H., van der Ploeg, R.R., 2006a. Trends in flood stages: contrasting results from the Mississippi and Rhine river systems. J. Hydrol. 331, 554–566.

Pinter, N., van der Ploeg, R.R., Schweigert, P., Hoefer, G., 2006b. Flood magnification on the River Rhine. Hydrol. Process. 20 (1), 147–164.

Rakhecha, P.R., Kennedy, M.R., 1985. A generalized technique for the estimation of probable maximum precipitation in India. J. Hydrol. 78, 345–359.

Rezacova, D., Pesice, P., Sokol, Z., 2005. An estimation of the probable maximum precipitation for river basin in the Czech Republic. Atmos. Res. 77, 407–421.

Salzgitter Industriebau GmbH, 1963. Nam Pong Project Engineering Report, Part II Hydrology, Western Germany, North-East Electricity Authority, Bangkok Thailand.

Salzgitter Consult GmbH, Team Consulting Engineers, Asian Institute of Technology, 1983. Ubol Ratana Dam Flood Protection Study, Final Report, Electricity Generating Authority of Thailand.

Samuel, J.M., Sivapalan, M., 2008. Effects of multiscale rainfall variability on flood frequency: comparative multisite analysis of dominant runoff processes. Water Resour. Res. 44, W09423. http://dx.doi.org/10.1029/2008WR006928.

Sivapalan, M., Blöschl, G., Zhang, L., Vertessy, R., 2003. Downward approach to hydrological prediction. Hydrol. Process 17, 2101–2111. http://dx.doi.org/10.1002/hyp.1425.

Sivapalan, M., Wood, E.F., Beven, K.J., 1990. On hydrologic similarity, 3. A dimensionless flood frequency model using a generalised geomorphic unit hydrograph and partial area runoff generation. Water Resour. Res. 26 (1), 43–58.

Syvitski, J.P.M., Brakenridge, R.G., 2013. Causation and avoidance of catastrophic flooding along the Indus River, Pakistan. GSA Today 23 (1), 4–10.

Taesombut, V., 2001. Potential Flood Control of Upper Chao Phraya by Large and Medium Reservoirs, Research Report for National Research Council of Thailand (in Thai).

Tamai, N., 1992a. Discharge prediction for flow in a compound channel: a new approach to overbank flow, Part 1: Evaluation of floodplain resistance. Civil Eng. Trans., Inst. Engrs. Aust. CE34 (4), 285–294.

Tamai, N., 1992b. Discharge prediction for flow in a compound channel: a new approach to overbank flow, Part 2: Discharge prediction based on a depth-averaged flow equation. Civil Eng. Trans., Inst. Engrs. Aust. CE34 (4), 295–302.

Thanapakpawin, P., Richey, J., Thomas, D., Rodda, S., Campbell, B., Logsdon, M., 2006. Effects of landuse change on the hydrologic regime of the Mae Chaem river basin, NW Thailand. J. Hydrol. 334, 215–230.

United States Department of the Interior, Bureau of Reclamation, 1974. Design of Small Dams, 2nd ed., Oxford & IBH Publishing CO.

US Department of Commerce and US Department of the Army, 1970. Probable Maximum Precipitation, Mekong River Basin, Hydrometeorological report No.46.

Viglione, A., Castellarin, A., Rogger, M., Merz, R., Blöschl, G., 2012. Extreme rainstorms: comparing regional envelop curves to stochastically generated events. Water Resour. Res. 48 (1). http://dx.doi.org/10.1029/2011WR010515.

Wittenberg, H., 1994. Nonlinear analysis of flow recession curves. IAHS Publ. 221, 61–67.

Woltemade, C.J., Potter, K.W., 1994. A watershed modeling analysis of fluvial geomorphologic influences on flood peak attenuation. Water Resour. Res. 30, 1933–1942.

Wood, E.F., Sivapalan, M., Beven, K., 1990. Similarity and scale in catchment storm response. Rev. Geophys. 28, 1–18.

World Meteorological Organization, 1986. Manual for Estimation of Probable Maximum Precipitation, WMO-No.332, Second Edition.

Wormleaton, P.R., Merrett, D.J., 1990. An improved method of calculation for steady uniform flow in prismatic main channel/flood plain sections. J. Hydraul. Res. 28 (2), 157–174.

Zielinski, P.A., 2011. Inflow design flood and dam safety. Proceedings of the International Symposium on Dams and Reservoirs Under Changing Challenges – 79 Annual Meeting of ICOLD, Swiss Committee on Dams, pp. 677–684.